International Journal of Crashworthiness
Publication details, including instructions for authors and subscription information:
http://www.informaworld.com/smpp/title~content=t778188386

Crash performance of X-shaped support base work zone temporary sign structures

Junwon Seo [a]; Daniel G. Linzell [b]; Zoltan Rado [c]
[a] Department of Civil and Environmental Engineering, The Pennsylvania State University, University Park, PA [b] Department of Civil Engineering, The Pennsylvania State University, University Park, PA [c] Crash Safety Research Center, The Pennsylvania Transportation Institute, University Park, PA

Online Publication Date: 01 August 2008

To cite this Article Seo, Junwon, Linzell, Daniel G. and Rado, Zoltan(2008)'Crash performance of X-shaped support base work zone temporary sign structures',International Journal of Crashworthiness,13:4,437 — 450
To link to this Article: DOI: 10.1080/13588260802221393
URL: http://dx.doi.org/10.1080/13588260802221393

International Journal of Crashworthiness
Vol. 13, No. 4, August 2008, 437–450

Taylor & Francis
Taylor & Francis Group

Crash performance of X-shaped support base work zone temporary sign structures

Junwon Seo[a], Daniel G. Linzell[b,*] and Zoltan Rado[c]

[a]*Department of Civil and Environmental Engineering, The Pennsylvania State University, University Park, PA;* [b]*Department of Civil Engineering, The Pennsylvania State University, University Park, PA;* [c]*Crash Safety Research Center, The Pennsylvania Transportation Institute, University Park, PA*

(*Received 17 December 2007; final version received 22 May 2008*)

Results from numerical analyses of temporary sign structure crash tests are compared with test data to assess both their crashworthiness and numerical model effectiveness. In addition, a parametric study is performed to investigate the influence of various parameters that would affect crash performance. Sign structures supported with an X-shaped base configuration in plan ('X-base') were examined, with all tests being performed following National Cooperative Highway Research Program (NCHRP) 350, 'Recommended Procedures for the Safety Performance Evaluation of Highway Features' guidelines [16]. Simulations and tests were completed at a speed of 98.7 km/h (61.3 mph) as directed by NCHRP 350 with the signs oriented perpendicular and parallel to the vehicle's direction of travel. Results from the study indicated that numerical simulations properly predicted the crash behaviour. In addition, both the numerical model and crash tests showed that orienting the X-base structure parallel to the vehicle direction would result in sign penetration into the vehicle compartment and, subsequently, an unsatisfactory condition according to NCHRP 350.

Keywords: crash test; crash performance; numerical simulations; temporary sign structure

Introduction

The number of fatalities on public roadways in the United States reached a recent high of about 42,000 [13]. A significant number of those fatalities occur in work zones [5]. As a result, safety of all persons within the work zone is of crucial importance. One of the most effective methods to ensure work zone safety is the utilisation of a number of temporary sign structures for drivers approaching and passing through the zone [5]. However, should a vehicle stray off course and impact a temporary sign, both the sign and supporting structure could become a safety threat, especially to persons within the vehicle compartment. Therefore, there is a need for crash testing so that a level of confidence and safety can be established for persons within vehicles for the myriad of work zone sign designs that are being used.

As a result of the need for evaluating the crash effectiveness of various types of signs, including work zone sign structures, various publications and guidelines have been developed. The most comprehensive publication is National Cooperative Highway Research Program (NCHRP) Report 350, titled *Recommended Procedures for the Safety Performance Evaluation of Highway Features*, completed by the Texas Transportation Institute in 1993 [16]. NCHRP 350 formed the basis for the evaluation of all transportation sign structures, including the temporary sign structures discussed herein. Full-scale crash studies of sign structures were used for the development of NCHRP 350 [14]. Temporary sign specimens that were tested were limited to breakaway bases fabricated using steel support posts embedded in a concrete foundation.

A number of studies have been published on temporary sign structure crash test performance outside the NCHRP 350 work. Bligh et al. [2] provided temporary sign structures for use in work zones that would perform satisfactorily when impacted by errant vehicles in accordance with national safety performance guidelines set forth in NCHRP 350 [14]. Bligh et al. [3] and Mak et al. [9] designed, evaluated and tested additional work zone sign supports that would perform satisfactorily when impacted by errant vehicles. The researchers conducted a total of 12 crash tests on various work zone traffic-control devices, including a portable sign support, a skid-mounted sign support and three vertical panel supports. Mak et al. [8] and Polivka et al. [15] also assessed the impact performance of various work zone traffic-control devices, including temporary sign supports, plastic cones, vertical panels and barricades. Ross et al. [17] reported on crash tests of single-post roadside signs. This work evaluated the performance of the stub-sign post system base using full-scale crash tests. Breaux and Morgan [4] completed an extensive study of small signs and sign support systems used by federal, state and local agencies. This work showed that most sign

*Corresponding author. Email: dlinzell@engr.psu.edu

ISSN: 1358-8265

DOI: 10.1080/13588260802221393
http://www.informaworld.com

systems, breakaway or not, followed a linear kinetic energy and impact velocity relationship. It stated that the estimated changes in velocity could be useful for recertification of existing sign systems as well as for extrapolation from single to multiple post systems.

Other temporary work zone protection systems have been crash tested and reported more extensively, such as concrete barrier systems. Atahan [1] tested the New York Department of Transportation Portable Concrete Barriers (NYPCB) and evaluated their performance in accordance with NYPCB design criteria. A finite-element representation of the tested barrier system was developed using LS-DYNA [7]. Validated LS-DYNA numerical simulations of low-profile portable concrete barrier systems used for work zones were also used to assist with the conceptual development of a new temporary concrete barrier system [6].

The Federal Highway Administration (FHWA) through its *Manual on Uniform Traffic Control Devices* states that all temporary work zone traffic control devices must meet crash testing requirements from NCHRP 350 (1, 16. NCHRP 350 requires that crash tests be conducted using an 820C vehicle (820-kg compact car) with tests completed for signs oriented at critical angles relative to the vehicle's

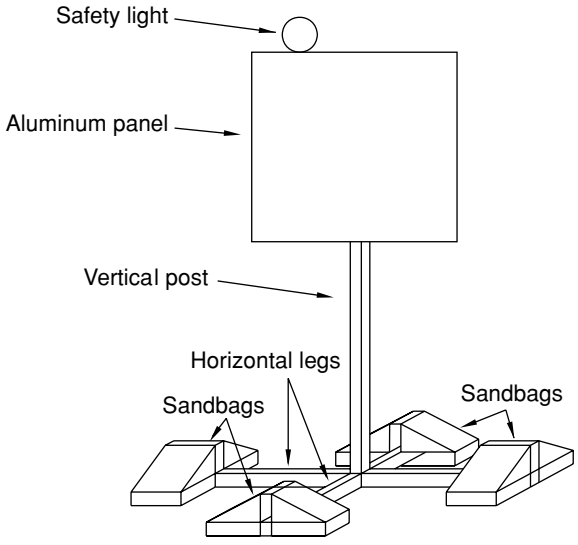

(a) Sign configuration

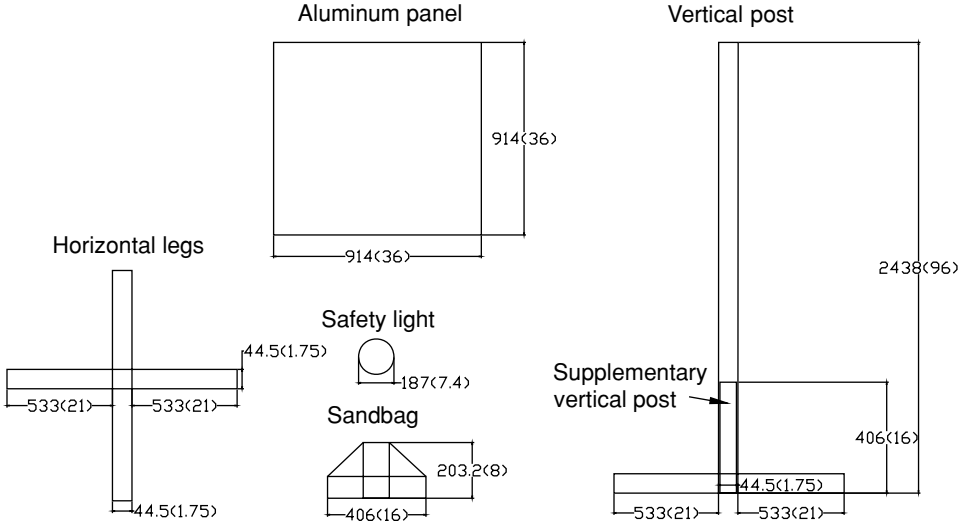

(b) Sign component details, unit: mm (in)

Figure 1. X-base sign.

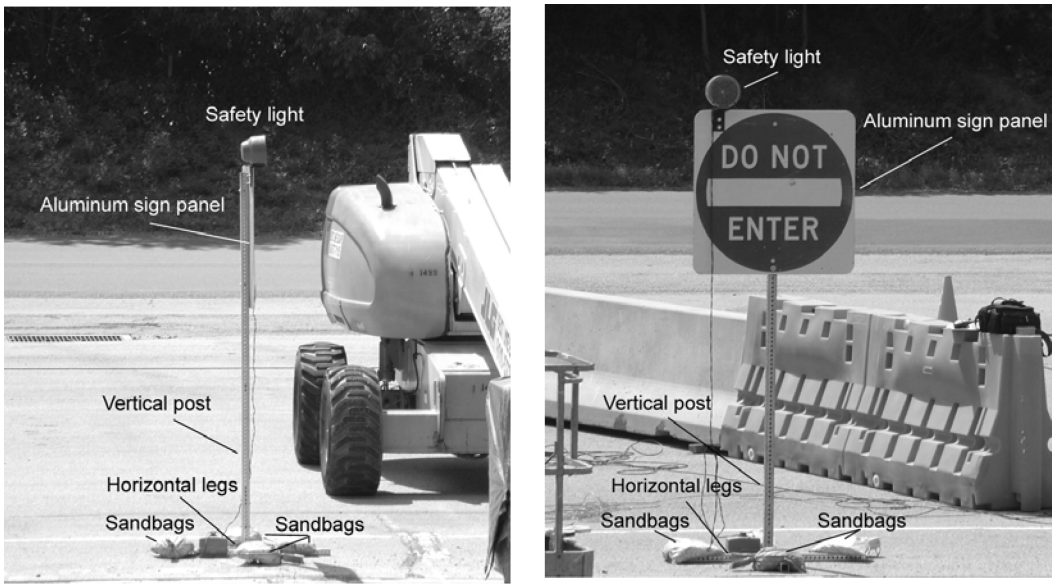

(a) 0 degree impact angle (perpendicular) **(b) 90 degree impact angle (parallel)**

Figure 2. Examined X-base sign orientation relative to traffic direction.

direction of travel. It also states that finite-element simulations can help evaluate crash performance at a reduced cost.

Therefore, this article is intended to summarise the work completed in conjunction with a project investigating temporary sign crashworthiness using finite-element simulations and full-scale tests. Crash testing criteria for the temporary sign structure investigated herein both numerically and using full-scale tests was established following NCHRP 350. A Geo Metro was used for the 820C vehicle tests, and the temporary sign structure was supported using an X-shaped base in plan (Figure 1), a design common in Pennsylvania and described in detail in the following section. This structure was oriented with the sign face perpendicular and parallel to the vehicle direction with tests completed at a speed of 98.7 km/h (61.3 mph). Results from numerical simulations using LS-DYNA and actual crash tests are presented, compared and evaluated.

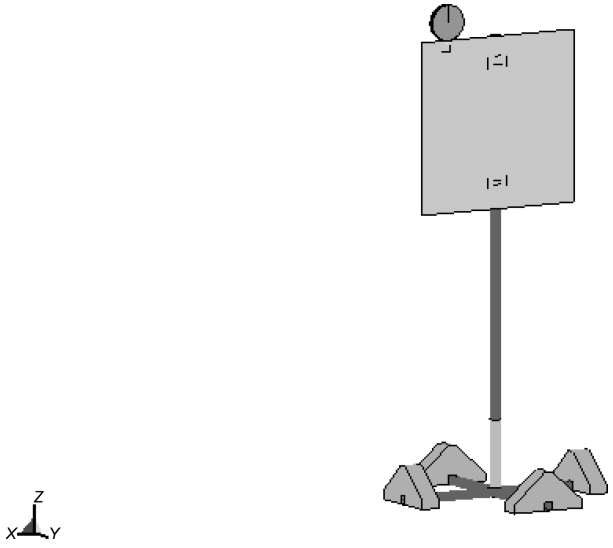

Figure 3. X-base sign structure LS-DYNA.

X-base structure

A typical X-base temporary sign support consists of an aluminium sign panel hung from a steel vertical upright post and supporting legs as shown in Figure 1. Typically, these structures have sandbags placed onto their legs to provide stability and a safety light at the top of sign panel. A representative sketch of a typical X-base structure, including sandbags and a safety light, is shown in Figure 1. Representative photos are shown in Figure 2.

The sign's horizontal support legs consist of ASTM A500 Grade B steel tubes that are 44.5 mm (1.75 in) ×

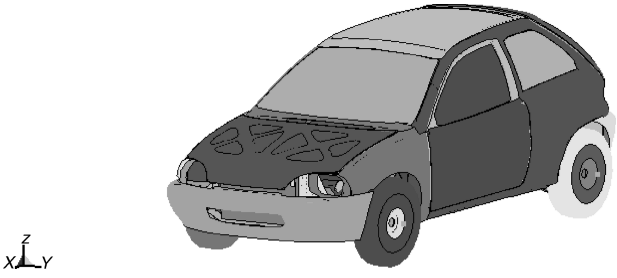

Figure 4. Geo Metro LS-DYNA [4].

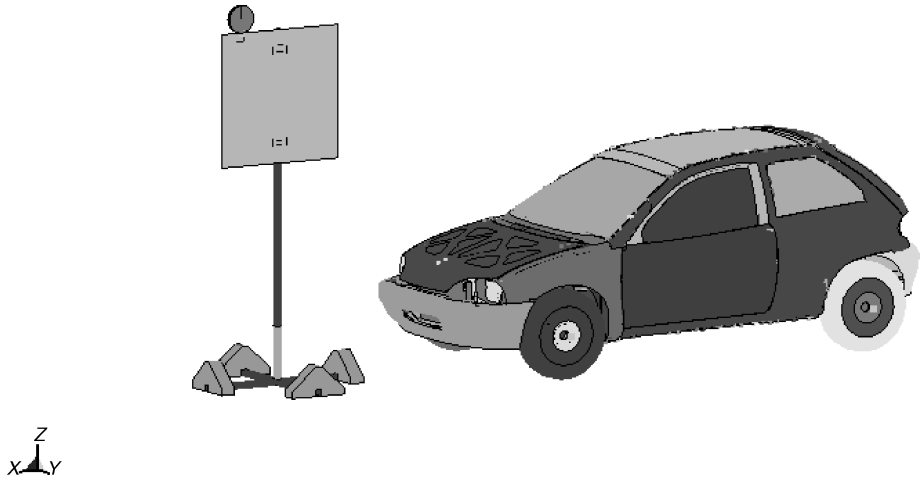

Figure 5. Representative numerical crash test.

44.5 mm (1.75 in) × 2.78 mm (0.11 in) thick. The crossing legs used for the X-shaped base are both 1111.3 mm (43.8 in) in length. The aluminium sign panel hung from the support is 914.4 mm (36 in) × 914.4 mm (36 in) square × 5.54 mm (0.2 in) thick. The sign panel is rigidly bolted to the vertical post made of ASTM A500 Grade B steel tubing. The vertical post is 50.8 mm (2 in) × 50.8 mm (2 in) square × 2.78 mm (0.11 in) thick and 2438.4 mm (96 in) in height. The sandbags used for temporary stabilisation of portable sign structure are placed on each of the four horizontal legs as shown in Figure 1a. Each sandbag is 406.4 mm (16 in) wide × 203.2 (8 in) mm in height × 101.6 mm (4 in) in length. The safety light has a radius of 187.3 mm (7.4 in) and is positioned on top of the sign. Bolts that attached the sign panel to the vertical post are made of aluminium and are fully threaded. The diameter of each head and thread is 12 mm (0.47 in) and 7 mm (0.28 in). The bolt length is 65 mm (2.56 in). As stated in the Introduction section, two sign orientations relative to the vehicle direction were tested as shown in Figure 2.

Numerical modelling

The temporary sign structures and 820C vehicle were modelled and virtual crash testing was performed using LS-DYNA, an explicit non-linear finite-element analysis code. LS-DYNA has been effectively used to analyse crash performance for other work zone devices [1, 6]. Modelling decisions are specified as follows.

Temporary sign

The steel legs and posts and the aluminium sign panel were modelled using quadrangle-shaped shell elements available in LS-DYNA which have an element formulation as shown in Equation 1 below [7].

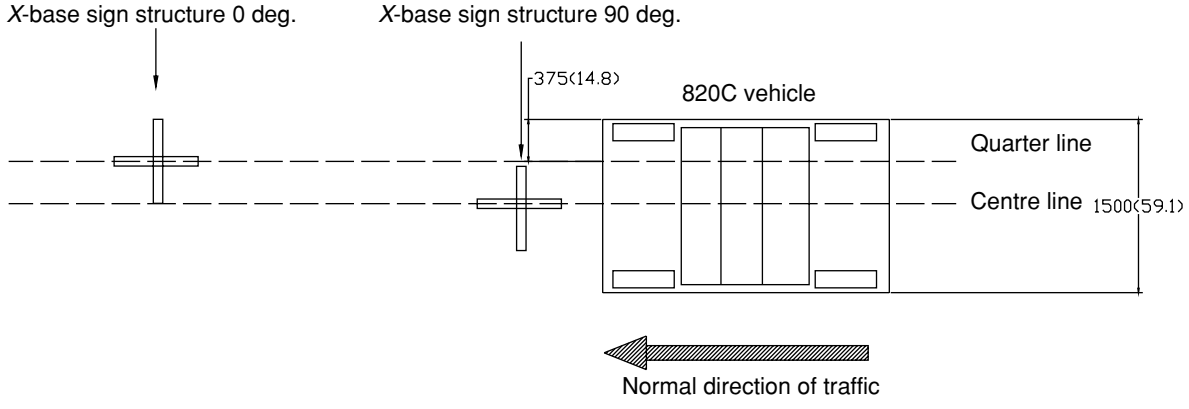

Figure 6. Crash testing layout, mm (in).

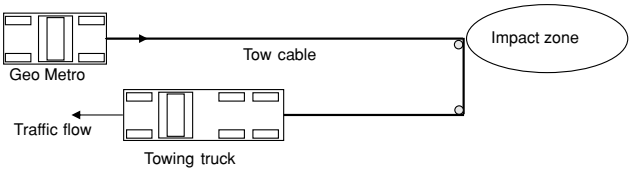

Figure 7. Crash testing configuration.

$$x^m = N_I(\xi, \eta)x_I \tag{1}$$

where the subscript I is summed over all nodes and $N_I(\xi, \eta)$ is a bilinear shape function. Each wall of the tubular steel legs and posts was represented using these shell elements. To account for weight effects of the sandbags and warning light, they were modelled using eight-noded hexahedron solid elements which have the element formulation shown in Equation 2 [7].

$$x_i(X_\alpha, t) = x_i(X_\alpha, (\xi, \eta, \zeta), t) = \sum_{j=1}^{8} \phi_j(\xi, \eta, \zeta)x_i^j(t) \tag{2}$$

The shape function ϕ_j is defined for the eight-node hexahedron as

$$\phi_j = \frac{1}{8}(1 + \xi\xi_j)(1 + \eta\eta_j)(1 + \zeta\zeta_j) \tag{3}$$

where $\xi_j\eta_j\zeta_j$ take on their nodal values of $(\pm1, \pm1, \pm1)$, and x_i^j is the nodal coordinate of the jth node in the ith direction. The light 340 g (12 oz) was modelled using mass elements available in LS-DYNA program and matching standard, published dimensions as shown in Figure 1b. The 340 g (12 oz) of light weight was calculated on the basis of its geometric properties, and the density of plastic and was placed onto the top of sign panel as shown in Figure 3. Each 22.5-kg (50 lb) sandbag was placed onto the legs.

Nominal material properties were used for the ASTM A500 Grade B steel and the aluminium alloy. Inelastic effects were addressed using the piecewise linear plasticity function available in LS-DYNA. This function allows for the definition of eight points along the stress-strain curve, with these points being obtained from nominal stress-strain curves for each material. Nominal geometric properties by PennDOT and shown in Figure 1b were also used.

The sign panel was separately modelled from the support structures and connections between the two were accomplished using *Constrained Spot Welds* provided by LS-DYNA. *Constrained Spot Welds* couple nodes together via nodal forces and were used to represent the capacity of the bolts that connected the actual sign and support structure components together through specified normal and shear force capacities at the spot weld. The failure criterion used by the LS-DYNA *Constrained Spot Welds* is based on a least squares algorithm and appears as shown in Equation 4 [7].

$$\left(\frac{|f_n|}{S_n}\right)^n + \left(\frac{|f_s|}{S_s}\right)^m \geq 1 \tag{4}$$

where f_n and f_s are the normal and shear forces at the interface; n and m are assigned exponents for the normal and shear spot weld forces; and S_n and S_s are normal and shear forces at spot weld failure. Values of n and m equal to 2 were selected for spot welds that represented the sign and support connections because failure at this location could include both plastic and brittle components. An isometric view of the completed LS-DYNA sign model is shown in Figure 3.

Friction between the sign base and infinitely stiff surface representing the earth was modelled using a Coulomb friction model [7]. For this model, the coefficient of friction, μ was set at 0.3 because previous research indicated that using coefficients of friction between 0.3 and 0.35 successfully represented actual crash test frictional forces [1,10]. The portion of the structure in contact with the ground was preloaded with the solid elements representing the sandbags prior to vehicular impact, and the coefficient of friction between the sandbags and the legs was also set equal to 0.3.

Vehicle

A standard NCHRP-approved vehicle model developed by the National Crash Analysis Center (NCAC) was used for the numerical crash testing [12]. The LS-DYNA finite-element model of an 820C vehicle (i.e. an 820-kg

Table 1. Final test matrix for portable sign support [16].

Test level	Feature	Test designation	Impact conditions		
			Vehicle	Nominal speed, km/h (mile/hr)	Nominal angle (°)
3 Basic level	Support structures	Test 3–61	820C	100 (62.14)	0–90
	Work zone traffic control devices	Test 3–71	820C	100 (62.14)	0–90

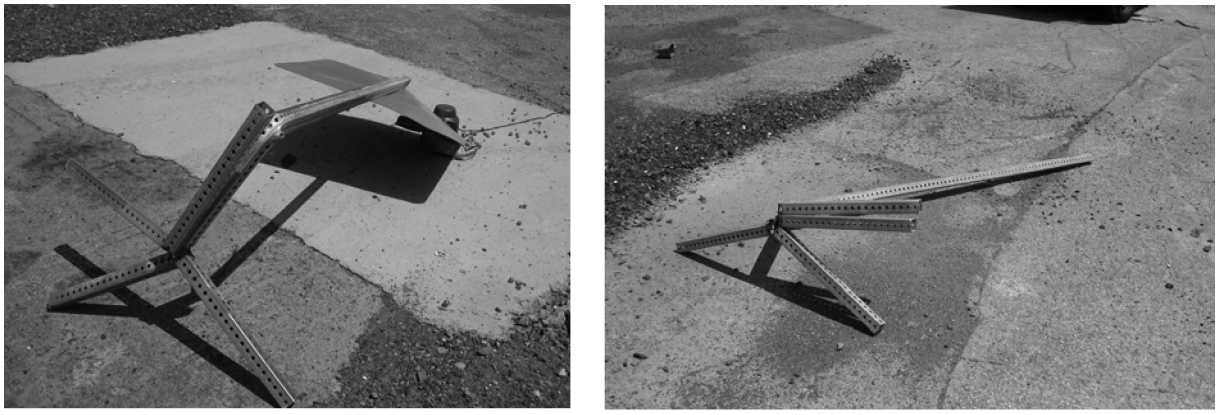

(a) 0 degrees (perpendicular) **(b) 90 degrees (parallel)**

Figure 8. Crash performances for X-base sign structures.

(1808-lb) compact car) was incorporated into the numerical crash testing analyses. Car model elements are divided into spring, mass and solid elements. The spring elements were used for generation of dampers, the mass elements to represent weights of each vehicle component and the solid elements to represent the wheels, roof, doors and other components of the car. An isometric view of the NCAC 820C vehicle finite-element model is shown in Figure 4. A similar car was used for actual crash testing. The numerical car contained a crash 'dummy' with weights that matched the dummy used for actual testing. Influence of the sandbags coupled with changes to vehicle response and the possibility of sign intrusion into the passenger prompted the use of a crash dummy for both the real and numerical crash tests. For a small car, NCHRP 350 requires using a dummy to achieve a gross static weight of 895 ± 25 kg (1973.5 ± 55.1 lb), and for this test, a 75-kg (165.4-lb) dummy was asymmetrically placed within the vehicle. The inertial properties of the car are influenced to a relatively large degree by the use of this dummy along with the impact dynamics and characteristics and vehicle post-impact trajectory. Response of this dummy during the test was used to evaluate crash testing performance numerically following NCHRP 350 criteria.

Virtual crash testing

Crash scenarios were selected following NCHRP 350 criteria after consulting with an official from the Federal Highway Administration Office of Safety Design – HSSD. Using appropriate test matrices from NCHRP 350, it was decided in cooperation with the FHWA official to employ level-3 test requirements from the 'Support Structures' category with Test 3–61 and from the 'Work Zone Traffic Control Devices' category with Test 3–71 as a supplemental reference. The final test matrix is shown in Table 1.

Test 3–61 comprised two separate full-scale crash scenarios at approximately 98.7 km/h (61.3 mph) with the 820C vehicle using sign-impact angles of 0° (perpendicular) and 90° (parallel) relative to the normal traffic direction. Each crash scenario was analysed twice in LS-DYNA following NCHRP 350 criteria, once with the sign structure impacting the vehicle's front at its longitudinal centreline and once with the sign structure impacting the front at the mid-point between the vehicle's longitudinal centreline and its outer edge. Figure 5 shows a representative numerical crash test at impact angles of 90°.

Numerical crash tests followed a specified sequence. Both the sign and vehicle models were placed onto the rigid surface representing the ground. The sign models were placed at their correct position relative to the vehicle longitudinal centreline and were initially located approximately 1 m (0.3 ft) in the direction of traffic away from the vehicle. A velocity of 98.7 km/h (61.3 mph) was instantaneously imposed on the vehicle by setting the rotational speed of the tyres to match appropriate angular velocities to mitigate

Table 2. LS-DYNA simulation crash performance.

X-base support position	Vehicle speed, km/h (mph)	S_x, mm (in)	S_y, mm (in)	Maximum deformation, (in)	Maximum penetration, mm (in)
0°	98.7 (61.3)	18.0 (0.71)	0.0 (0.0)	160.9 (6.33)	1.8 (0.07)
90°	98.7 (61.3)	71.0 (2.80)	0.0 (0.0)	195.9 (7.71)	14.0 (0.55)

Figure 9. 820C vehicle crash performance.

differential frictional and inertial effects. At the completion of the virtual crash tests, maximum displacements and accelerations of the crash dummy were measured and used to evaluate crashworthiness.

Full-scale crash testing

The full-scale crash testing configuration is shown in Figure 6. Note that both the 0° and 90° sign orientations were impacted during a single test as recommended during the previously mentioned conversations with an FHWA official. The first X-base sign structure was placed in the longitudinal centreline of the approaching vehicle at a 90° angle while the second sign was placed one vehicle length behind the first at a 0° angle. The second impacted the mid-point between the centreline and vehicle edge.

0.1. Test vehicle and hardware

Crash testing was performed using an 820C vehicle at The Pennsylvania Transportation Institute (PTI) facility. A 1993 Geo Metro was used for the 820C vehicle crash test. The measured inertial mass of vehicle was 816 kg (1799 lb), while gross static mass was 891 kg (1964 lb). The PTI facility uses a rigid rail to provide vehicle guidance, a reverse towing system to accelerate the vehicle to the required test speed and a release mechanism that disconnects the tow cable prior to impact.

The PTI's rail guidance system consists of a 320 m (1050 ft) long, 8.89 cm (3.5 in) high I-beam (guide rail) and bogey assembly. The right (east) end of the rail terminates into the impact zone where the bogey is detached from the vehicle as shown in Figure 7. The rail is securely anchored to the pavement along the edge of the vehicle dynamics test pad, as is the bogey-arresting device. The bogey was attached to the undercarriage of the vehicle from the side.

The towing system was used to bring the test vehicle up to the measured 98.7 km/h (61.3 mph) impact speed. This system consists of a tow vehicle, a tow cable, two anchored re-directional pulleys, a speed multiplier pulley attached to the towing vehicle, and a quick-release mechanism anchored to the pavement.

Instrumentation and data acquisition

Test vehicles were instrumented with two tri-axial measurement systems designed to measure linear acceleration along three orthogonal axes and rotation rates around three orthogonal axes. The first system used three ±20 G accelerometers to measure longitudinal, lateral and vertical acceleration levels. The second system used three 1000 degree/s angular rate sensors to measure roll, pitch and yaw rates. The two systems were secured to the vehicles in a

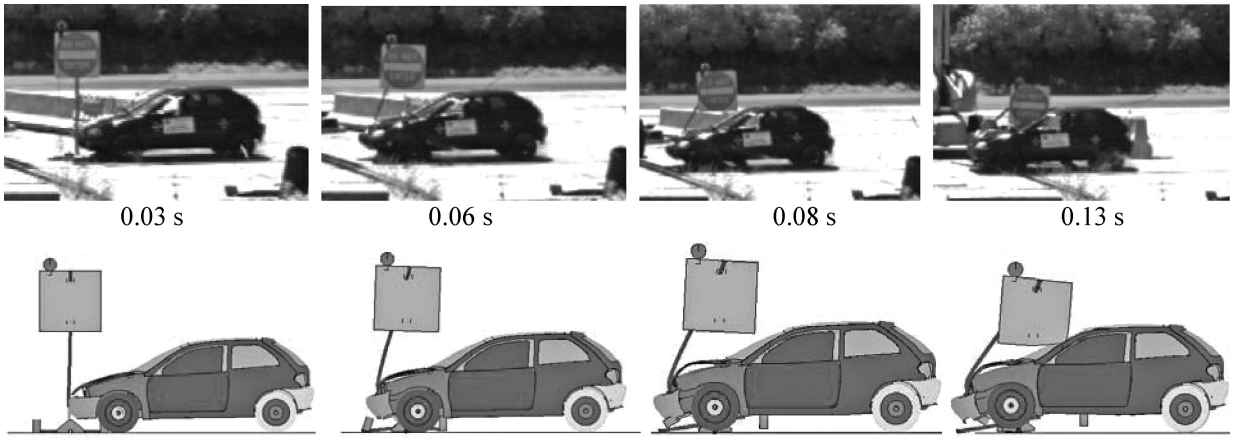

Figure 10. Crash snapshots and LS-DYNA simulations.

Table 3. Aggregate occupant risk factors and NCHRP evaluation limits.

Sign post name	Vehicle speed, km/h (mph)	Aggregate occupant impact velocity, m/s (ft/s)	Occupant ridedown acceleration, m/s^2 (ft/s^2)
0°	98.7 (61.3)	1.77 (5.81)	3.30 (10.83)
90°	98.7 (61.3)	1.79 (5.87)	3.61 (11.81)
NCHRP evaluation limits			
Preferred		3 (9.84)	5 (16.4)
Maximum		15 (49.2)	20 (164.0)

location near its centre of gravity. The vehicles were also instrumented with a Keyence PZ-61 photoelectric sensor to measure speed and an in-house impact sensor. Electronic signals from the accelerometers, rate, speed and impact sensors were recorded by an eight-channel TD data acquisition equipment certified to NHTSA, FAA, ISO 6487 and SAE J211 standards. Data collection was triggered at the release of the towing system. One-half second of pre-triggered data and eight seconds of post-triggered data were collected. Calibration and offset signals were also recorded before the test. The signals were sampled at 10 kHz and then filtered with a lowpass 100-Hz filter. The data

Table 4. Parametric study combinations.

	Parameters			
Combination	Weight of each sandbag, kg (lb)	Impact angle (°)	Speed, km/h (mph)	Coefficient of friction
1	12.5 (27.8)	0	100 (62.1)	0.3
2	22.5 (50.0)	0	100 (62.1)	0.3
3	32.5 (72.2)	0	100 (62.1)	0.3
4	22.5 (50.0)	0	100 (62.1)	0.3
5	22.5 (50.0)	30	100 (62.1)	0.3
6	22.5 (50.0)	60	100 (62.1)	0.3
7	22.5 (50.0)	90	100 (62.1)	0.3
8	22.5 (50.0)	0	35 (21.7)	0.3
9	22.5 (50.0)	0	50 (31.1)	0.3
10	22.5 (50.0)	0	75 (46.6)	0.3
11	22.5 (50.0)	0	100 (62.1)	0.3
12	22.5 (50.0)	0	100 (62.1)	0.3
13	22.5 (50.0)	0	100 (62.1)	0.5
14	22.5 (50.0)	0	100 (62.1)	0.7

Table 5. Parametric study crash simulation results.

	Assessment criteria							
Combination	Maximum Deformation, mm (in)		Maximum Penetration, mm (in)		Aggregate occupant impact, m/s (ft/s)		Occupant ridedown acceleration, m/s (ft/s)	
1	160.7	(6.3)	3.2	(0.1)	1.7	(5.7)	3.9	(12.62)
2	160.9	(6.3)	1.8	(0.1)	1.8	(5.8)	3.3	(10.82)
3	160.6	(6.3)	0.9	(0.0)	1.8	(5.7)	3.9	(19.74)
4	160.9	(6.3)	1.8	(0.1)	1.8	(5.8)	3.3	(10.82)
5	174.5	(6.9)	3.3	(0.1)	1.8	(5.8)	3.5	(11.57)
6	189.0	(7.4)	4.5	(0.2)	1.7	(5.4)	3.7	(18.85)
7	195.9	(7.7)	14.0	(0.6)	1.8	(5.9)	3.6	(11.84)
8	50.5	(2.0)	0.0	(0.0)	0.4	(1.4)	4.2	(17.18)
9	96.3	(3.8)	0.0	(0.0)	0.6	(2.0)	4.4	(14.30)
10	146.2	(5.8)	1.7	(0.1)	0.8	(2.7)	4.0	(12.98)
11	160.9	(6.3)	1.8	(0.1)	1.8	(5.8)	3.3	(10.82)
12	160.9	(6.3)	1.8	(0.1)	1.8	(5.8)	3.3	(10.82)
13	165.3	(6.5)	1.3	(0.1)	1.8	(5.9)	5.2	(17.09)
14	188.0	(7.4)	3.0	(0.1)	1.9	(6.1)	4.1	(13.49)

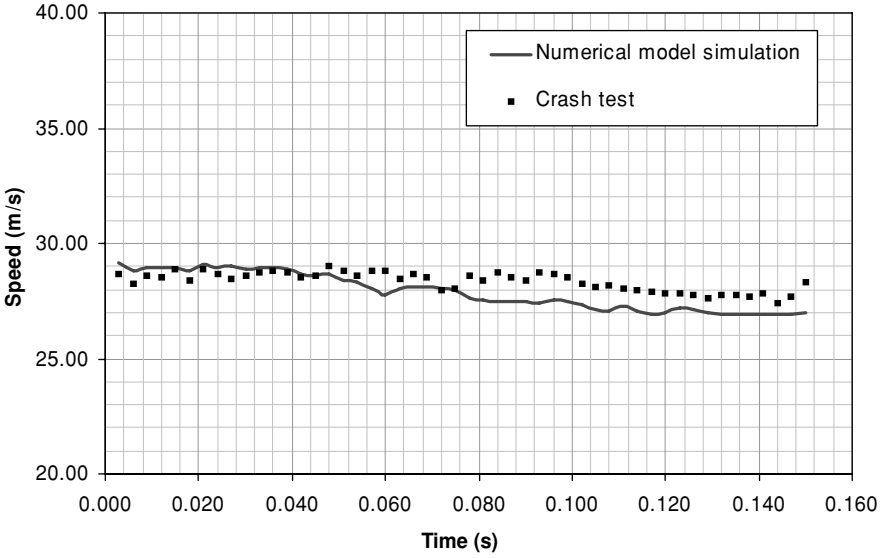

(a) Speed versus time history comparison

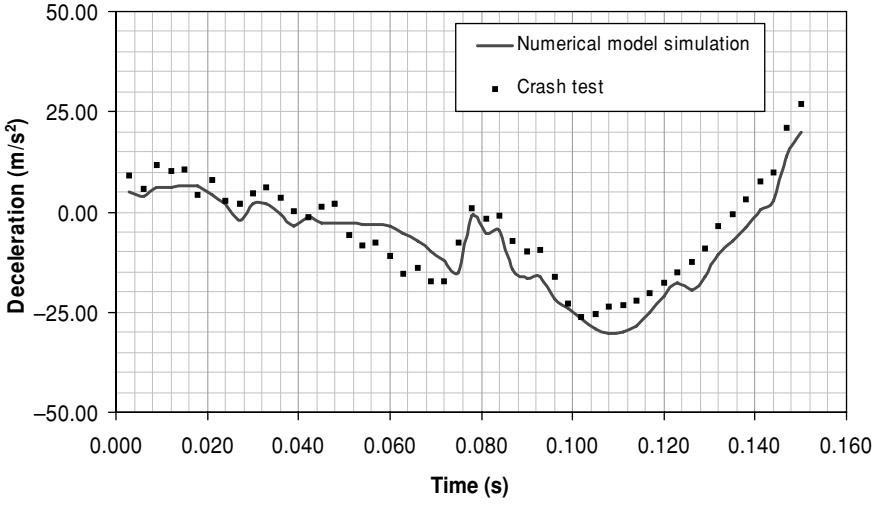

(b) Deceleration versus time history comparison

Figure 11. X-base sign crash testing and numerical simulation.

was downloaded to a notebook computer after the test for analysis.

High-speed digital video was recorded following NCHRP 350 requirements for post-test analyses, which included vehicle speed prior to impact, angle at impact, point of impact to the vehicle, and the exit speed for the vehicle. This video was also utilised to analyse the performance of the two X-base structures. Three additional high-speed video imaging systems were set up to provide additional test coverage and two more real-time video camera systems were used to supplement the high-speed video coverage. Pre- and post-test conditions were documented with high-resolution digital still cameras and a real-time video camera.

Crash performance

Sign and vehicle crash performance was visually addressed through crash and post-crash images. In addition, crash performance from LS-DYNA simulations and full-scale crash testing were compared and assessed following evaluation criteria from NHCRP 350.

Post-crash performance photographs are shown in Figure 8a. Figure 8a shows that the 0° X-base structure was severely deformed approximately 43.2 cm (17 in) in height above the ground, which was approximately equal to the front-bumper height. It can be seen that horizontal legs were also severely deformed at their connection joint. Figure 8b shows that the 90° structure was also severely deformed at approximately the same location.

In particular, for the 90° structure, the sign panel was totally separated from vertical post after the two connection bolts failed at impact. Figure 9 shows that the 820C vehicle was also extensively damaged with the front windshield and bumper fractured and the roof severely deformed.

Actual crash performance was well predicted from the LS-DYNA simulations both qualitatively and quantitatively. Figure 10 contains sequential snapshots of the impact from the 90° full-scale test and compares them qualitatively to the LS-DYNA model. Good correlation is observed, especially at the sign connections to the post that were modelled using the Constrained Spot Welds. The lower bolted connection in the actual sign failed at impact (0.03 s) while the upper bolt did not fail until 0.13 s, instances that were accurately predicted with the LS-DYNA simulation. This connection failure sequence rotated the sign panel clockwise and caused it to hit the windshield and vehicle roof, resulting in most of the damage.

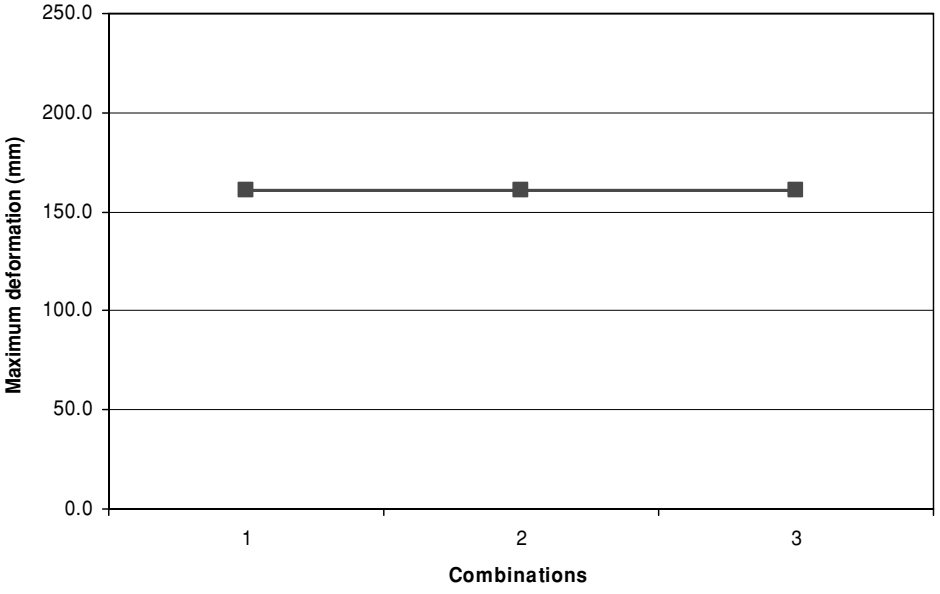

(a) Influence of sandbag weight (Combinations 1 to 3)

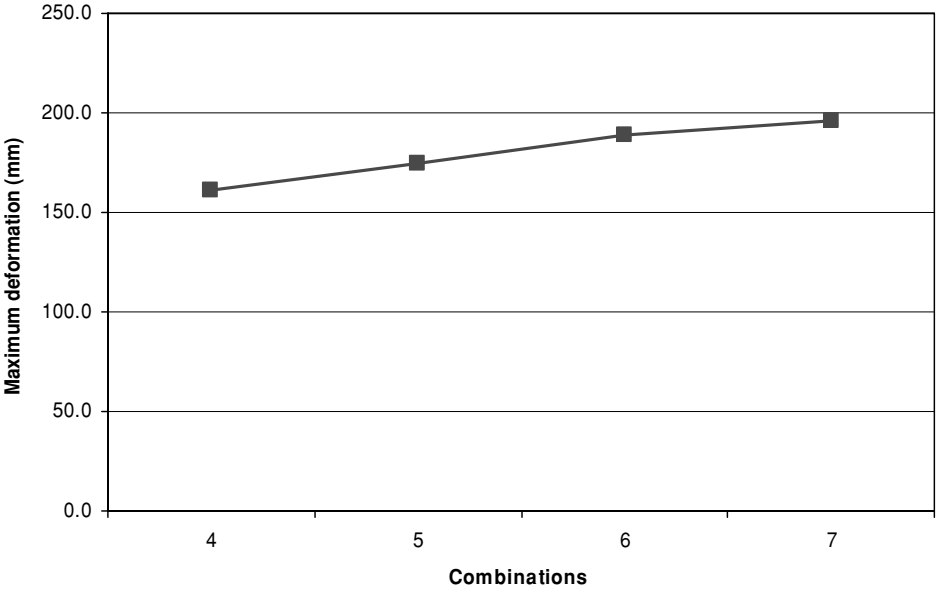

(b) Influence of impact angle (Combinations 4 to 7)

Figure 12. Maximum deformations for each combination. (*Continued*)

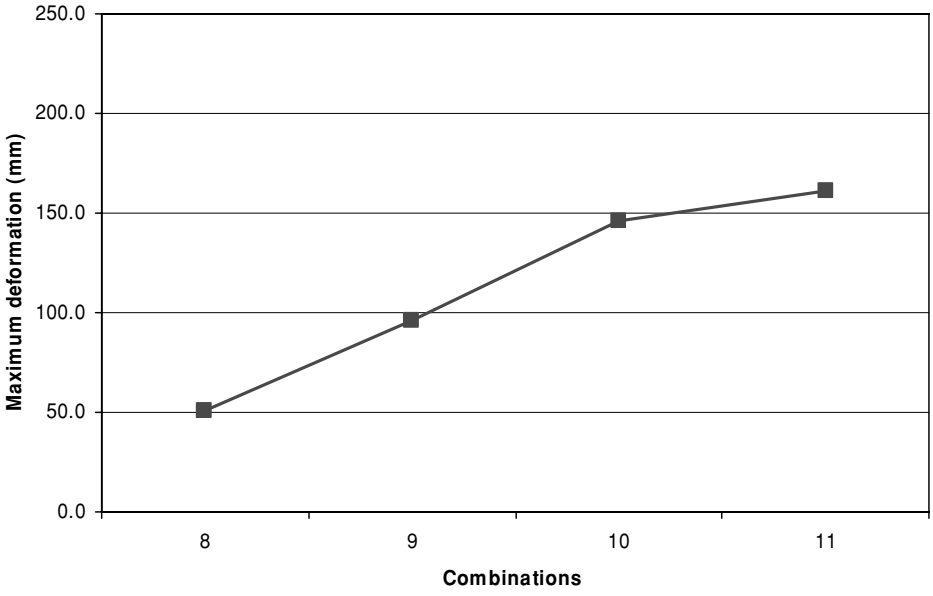

(c) Influence of vehicle speed (Combinations 8 to 11)

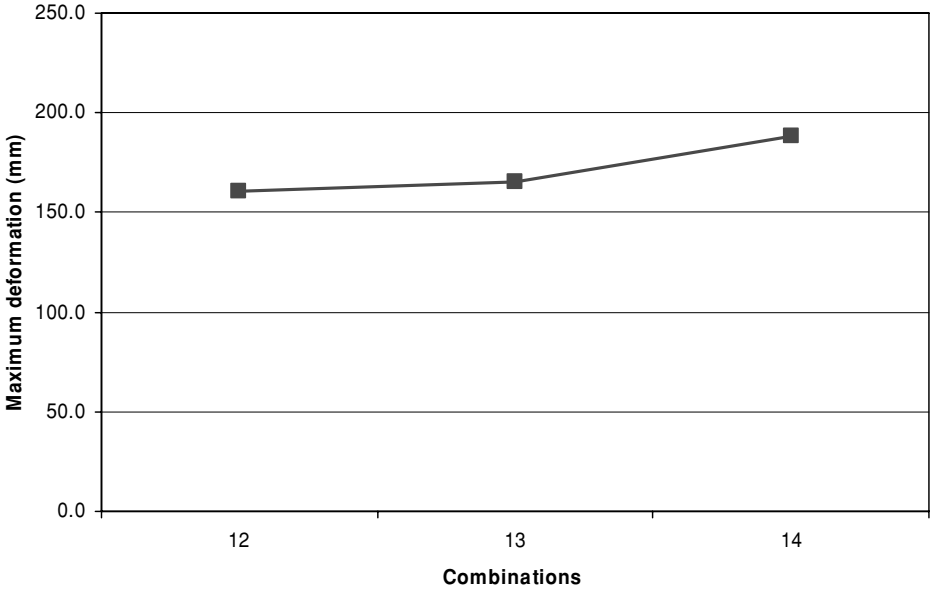

(d) Influence of coefficient of friction (Combinations 12 to 14)

Figure 12. (Continued)

The LS-DYNA simulations also adequately predicted speeds and deceleration quantities for the 820C vehicle throughout the crash test as shown in Figure 11. Figure 11a shows a representative speed time history comparison whereas Figure 11b shows a representative deceleration time history comparison. As seen in Figure 11a, speeds obtained from the numerical simulation and actual crash testing decreased slightly. Figure 11b shows that the LS-DYNA simulation did pick up the slight decelerations and accelerations of the vehicle well as it passed through the impact zone.

LS-DYNA simulations were used to evaluate X-base sign structure performance using NCHRP 350 criteria, with results for the two orientations being summarised in Table 2. S_x and S_y represent maximum displacements of the crash dummy within the vehicle at the end of the crash simulations in the global X and Y directions as shown in Figure 5. Maximum deformations shown in Table 2 are those at the front vehicle bumper with maximum penetration values being measured at the vehicle roof or the windshield. Table 2 indicates that the 90° test had much larger penetrations when compared with the 0° test, results

that were verified when actual crash testing images were examined.

An additional evaluation of crash performance occurred by utilising the simplified point mass Flail-Space Model from NCHRP 350 [16]. The Flail-Space model assumes that occupant injury severity is related to the velocity at which the occupant impacts the interior and the subsequent acceleration forces [11]. This model allows for the assessment of occupant risk during a crash event due to vehicular accelerations or decelerations. Two measures of risk were used: (1) the velocity at which a hypothetical occupant impacts a hypothetical interior surface, and (2) the ridedown acceleration subsequently experienced by the occupant. Aggregate occupant risk factors (i.e. the occupant impact velocity and occupant ridedown acceleration) in terms of the NCHRP 350 Flail-Space Model criteria were calculated. Table 3 shows the two aggregate occupant risk factors for the X-base structures. Acceptable and preferred limitations from NCHRP 350 for temporary support structures are given in Table 3 as well. It can be observed from the data that the X-base sign structures have delivered results that are within preferred NCHRP limitations.

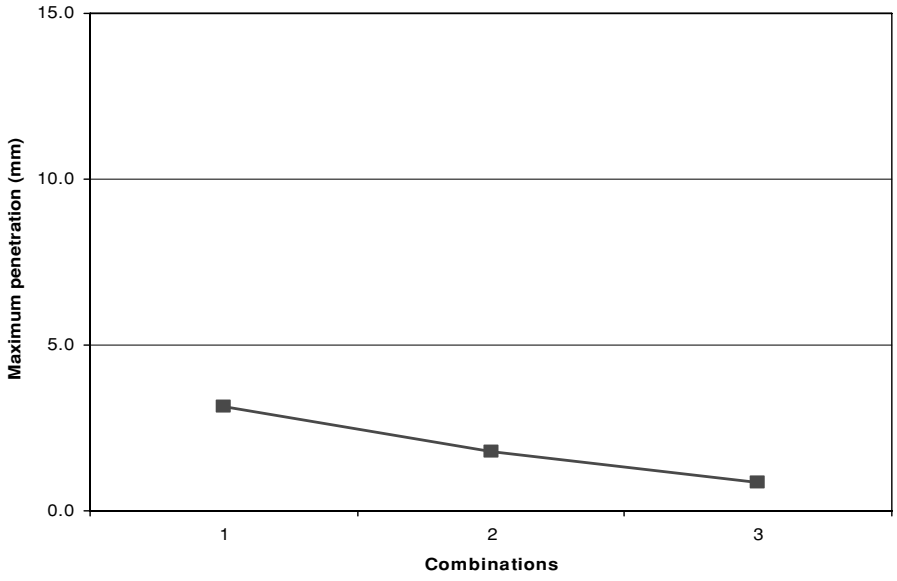

(a) Influence of weight of sandbags (Combination 1 to 3)

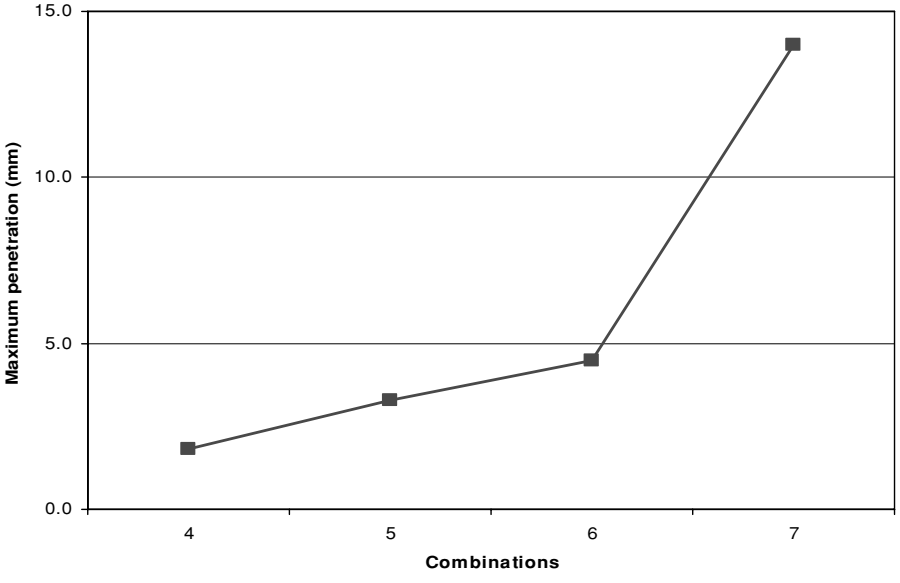

(b) Influence of impact angle (Combination 4 to 7)

Figure 13. Maximum penetrations for each combination. (*Continued*)

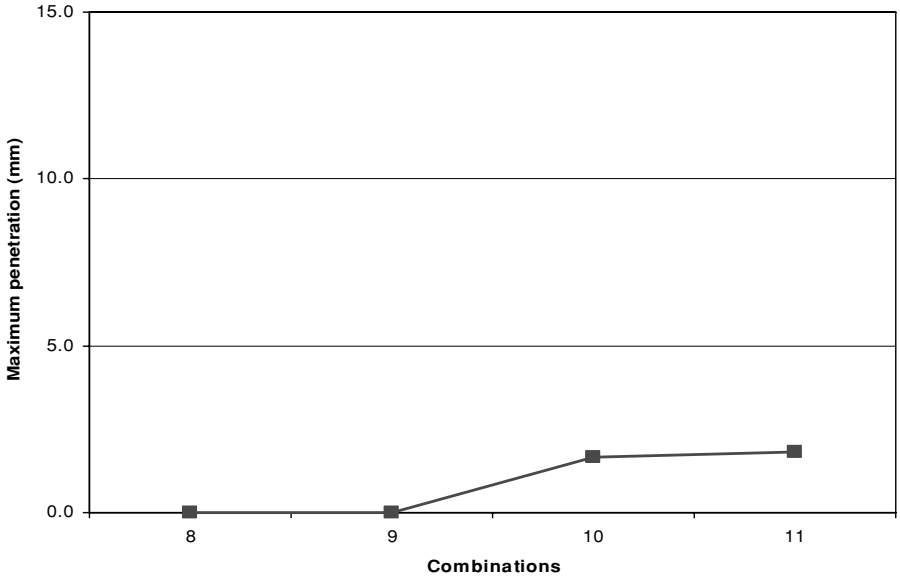

(c) Influence of vehicle speed (Combination 8 to 11)

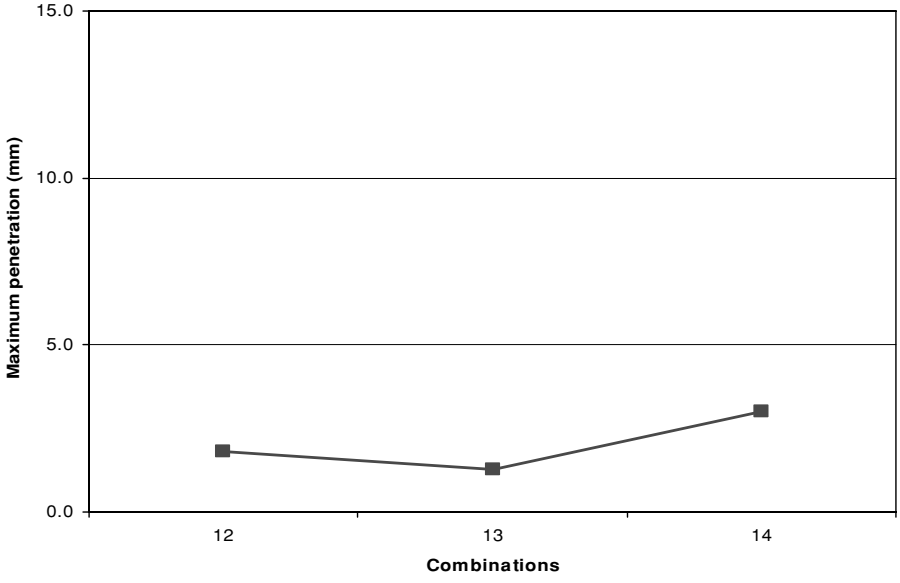

(d) Influence of coefficient of friction (Combination 12 to 14)

Figure 13. (Continued)

Parametric study

After validating the LS-DYNA crash simulations against actual test data, a parametric study was conducted to investigate the influence of select parameters that could have a significant effect on temporary sign crash performance. The selected parameters included: (1) sandbag weight, (2) vehicle impact angles, (3) vehicle speed, and (4) friction levels (Table 4). Each combination in Table 4 was examined numerically to ascertain the influence of one dominant parameter on crash performance. Combinations 1–3 examined sandbag weight, 4–7 impact angle, 8–11 vehicle speed, and 12–14 friction level.

Results from these examinations are shown in Table 5. Assessment criteria matched earlier discussions, with values corresponding to maximum deformations at the front of the vehicle, maximum penetration into the windshield, aggregate occupant impact measured by LS-DYNA software and occupant ridedown acceleration. Plots of the variation

of maximum deformation and maximum penetration as a function of the variation of each parameter detailed in Table 4 are shown in Figures 12 and 13. Table 5 indicates that, on the basis of the level of aggregate occupant impact and occupant ridedown accelerations, all parameter combinations for the X-base sign structure were within NCHRP limitations. Figures 12a and 13a show that sandbag weight had little influence on maximum deformation but did affect penetration by forcing the sign panel to rotate. Figures 12b and 13b indicate that impact angle had influence on maximum deformation and penetration because of impact eccentricity relative to the centre of gravity of the car. As expected, vehicle speed also had a significant influence on maximum deformation and penetration as shown in Figures 12c and 13c. Finally, as shown in Figures 12d and 13d, friction level had a reasonable influence on maximum deformation and penetration due to translational resistance provided by the ground.

Conclusions

Crash testing performance of two X-base temporary sign support structures was examined using full-scale testing and numerical simulations to assess the accuracy of the simulations and sign performance acceptability according to NCHRP 350 criteria. Crash response predictions from non-linear finite-element simulations in LS-DYNA were compared with full-scale crash test data. It was observed through these comparisons that LS-DYNA simulations replicated and predicted full-scale testing results (e.g. speeds, decelerations, etc.) in an efficient and cost-effective manner. Validated models were also used to evaluate crash performance in accordance with NCHRP 350 Flail-Space Model criteria. Results indicated that the X-base structures oriented both parallel and perpendicular to the vehicle satisfied Flail-Space Model requirements with respect to occupant velocities and accelerations/decelerations. However, the X-base structure oriented parallel to the vehicle did not satisfactorily meet NCHRP 350 evaluation criteria because penetration into the occupant compartment occurred. In addition, a parametric study was conducted to look at the influence of select parameters (e.g. sandbag weight, vehicle speed, impact angle and friction level) on crash performance using the validated models. It was observed via the parametric study that vehicle speed and impact angle, as expected, would be more influential factors affecting crash performance. It was also observed that, for the parameters that were selected and the crash tests that were simulated, all parameter combinations for the X-base sign structure were within NCHRP limitations.

Acknowledgements

The authors acknowledge the Pennsylvania Department of Transportation for funding this work.

References

[1] A.O. Atahan, *Finite-element crash test simulation of New York portable concrete barrier with I-shaped connector*, J. Struct. Eng. 132(3) (2006), pp. 430–440.

[2] R.P. Bligh, D.L. Bullard, W.L. Menges, and S.K. Schoeneman, *Impact performance evaluation of work zone traffic control devices*, Report 0-1792-2, U.S. Texas Transportation Institute, Texas, 2000.

[3] R.P. Bligh, K.K. Mak, and L.R. Rhodes, *Crash testing and evaluation of work zone barricades*, in *Transportation Research Record: Journal of the Transportation Research Board*, No. 1650, TRB, National Research Council, Washington, D.C., 1998, pp. 36–44.

[4] L.D. Breaux and J.R. Morgan, *Evaluation of small-sign systems from existing crash test data*, in *Transportation Research Record: Journal of the Transportation Research board*, No. 1258, TRB, National Research Council, Washington, D.C., 1990, pp. 13–22.

[5] M.A. Brewer, G. Pesti, and W. Schneider IV, *Identification and testing of measures to improve work zone speed limit compliance*. Report 0-4707-1, U.S. Texas Transportation Institute, Texas, 2005.

[6] G. Consolazio, J. Chung, and K. Gurley, *Impact simulation and full scale crash testing of a low profile concrete work zone barrier*, Comput. Struct. 81(13) (2003), pp. 1359–1374.

[7] LS-DYNA, *LS-DYNA Keyword User's Manual Version 970*, Livermore Software Technology Corporation, 2003. Available at http://www.lstc.com/manuals.htm.

[8] K.K. Mak, R.P. Bligh, and L. Rhodes, *Crash testing and evaluation of work zone traffic control devices*, in *Transportation Research Record: Journal of the Transportation Research Board*, No. 1650, TRB, National Research Council, Washington, D.C., 1998, pp. 45–54.

[9] K.K. Mak, R.P. Bligh, and W.L. Menges, *Evaluation of work zone barricades*. Report 7-3910-S, U.S. Texas Transportation Institute, 1997.

[10] D. Marzougui, G. Bahouth, A. Eskandarian, L. Meczkowski, and H. Taylor, *Evaluation of portable concrete barriers using finite element simulation*, FHWA Conference Presentation, Washington, D.C., 1998.

[11] J.D. Michie, *Collision risk assessment based on occupant flail-space model*, in *Transportation Research Record* 796, TRB, National Research Council, Washington, D.C., 1981, pp 1–9.

[12] NCAC. Available at http://www.ncac.gwu.edu/vml/models.html. Accessed 1 July 2007.

[13] *NHTSA Traffic Safety Facts*, NHTSA's National Center for Statistics and Analysis, 2005. Available at http://www.nhtsa.gov.

[14] R.M. Olson, *Development of safer roadside signs*, ASCE Environmental Engineering Conference, 6–9 February 1967.

[15] K.A. Polivka, R.K. Faller, J.R. Rohde, and D.L. Sicking, *Crash testing and analysis of work-zone sign supports*, in *Transportation Research Record: Journal of the Transportation Research Board*, No. 1797, TRB, National Research Council, Washington, D.C., 2002 pp. 96–104.

[16] H.E. Ross, Jr., D.L. Sicking, J.D. Zimmer, and R.A. Michle, *Recommended procedures for the safety performance evaluation of highway features*, National Cooperative Highway Research Program Report 350, Publication Project 22-7 FY'89, Texas Transportation Institute, Texas, 1993.

[17] H.E. Ross, M.J. Effenberger, and L.J. Sweeney, *Evaluation of bolted-base steel channel signpost*, in *Transportation Research Record: Journal of the Transportation Research Board*, No. 679, TRB, National Research Council, Washington, D.C., 1978, pp. 41–46.